

Article

Impact of Powdered Activated Carbon Structural Properties on Removal of Organic Foulants in Combined Adsorption-Ultrafiltration

Martin Schulz *, Sönke Bunting and Mathias Ernst 

Institute for Water Resources and Water Supply, Hamburg University of Technology,
Am Schwarzenberg-Campus 3, 20173 Hamburg, Germany; sonke@bunting.de (S.B.);
mathias.ernst@tuhh.de (M.E.)

* Correspondence: martin.schulz@tuhh.de; Tel.: +49-(0)-40-42878-3913

Received: 28 April 2017; Accepted: 31 July 2017; Published: 3 August 2017

Abstract: The impact of structural properties of three commercial PACs as well as two mechanically ground PACs on their efficiency in NOM removal and fouling reduction in combined adsorption-ultrafiltration (PAC-UF) of northern German groundwater was investigated. All PACs showed highest adsorption affinity for medium molecular weight NOM fractions. The meso-pore surface area rather than the total surface area (B.E.T.) mainly governed the extent of NOM removal. However, adsorption of macromolecular NOM fractions, which were found to be the main contributor to total and irreversible fouling, was limited by tested commercial carbons, and no significant mitigation of fouling was achieved by any tested PAC concentration. Lowering the particle size by grinding of the PAC, however, enhanced removal of macromolecular NOM fractions considerably, and fouling mitigation occurred at substantially lower PAC concentrations compared to raw carbons. A larger external surface area probably led to more shell adsorption, a more homogeneous particle distribution on the membrane surface and a better mass transport. In addition, comparison of the adsorption isotherms of raw and milled PACs showed that, due to the grinding of PAC particles, additional inner pores structures became available for NOM adsorption. Results of this study point out that structural properties of PAC dramatically influence the efficiency of combined PAC-UF, which needs to be considered during PAC selection and process design.

Keywords: powdered activated carbon (PAC); ultrafiltration (UF); membrane hybrid processes; NOM-removal; membrane fouling

1. Introduction

Natural organic matter (NOM) is ubiquitous in drinking water sources. In aquatic chemistry, the term “NOM” is used to designate all organic material in an aqueous ecosystem other than living organism and compounds of anthropogenic origin [1]. NOM originates from degradation of aqueous and terrestrial plants as well as from microbial excretion. It is a complex mixture of highly heterogeneous compounds including an infinite number of single compounds extremely difficult to identify. Therefore, it is common practice to classify groups of substances with similar properties, related to, e.g., size, hydrophobicity, and reactivity. NOM contains substances with a broad range of molecular weight, including macromolecular humic substances, polysaccharides and proteins, medium molecular amino sugars, peptides, lipids as well as small hydrophilic acids and neutrals. Furthermore, it consists of both hydrophobic components, including mainly aromatic carbon, with phenolic structures and conjugated double bonds as well as hydrophilic fractions, containing higher portions of aliphatic carbon and nitrogenous compounds [2].

The removal of NOM is a crucial step during drinking water treatment, since NOM can cause color, taste and odor problems [3], form disinfection by-products [4], mobilize heavy metals and other pollutants by complexation [5] and may lead to microbial regrowth in distribution systems [6]. In addition, especially macromolecular NOM fractions (e.g., humic substances, proteins, polysaccharides) were identified as main foulants during drinking water treatment by low-pressure membrane filtration [7,8]. Membrane fouling is the undesirable deposition of water constituents onto and into the membrane matrix, which leads to an increase of chemical cleaning frequency and operational costs while reducing membrane lifetime. Membrane fouling by NOM is governed by the characteristics of NOM molecules (size, charge, aromaticity, hydrophobicity), as well as by water chemistry (e.g., pH-value, ionic strength, divalent cations), membrane properties (e.g., pore size, charge, hydrophobicity) and applied operational conditions (e.g., flux/pressure, backwash frequency) [7–13]. Even though membrane fouling has been investigated in multitudes of studies during the last decades, it is still the main limitation during the application of low-pressure membrane processes and prevents their widespread use.

One option to effectively remove NOM during drinking water treatment is adsorption onto activated carbon [14]. Generally, NOM adsorption has been found to increase with decreasing pH and temperature, with increasing concentrations of divalent cations and dissolved oxygen, while removability by activated carbon adsorption tends to increase with decreasing molecular weight, increasing aromaticity and hydrophobicity [5,14,15]. Several studies focused on the implementation of powdered activated carbon (PAC) in low-pressure membrane systems (microfiltration (MF), UF) and proved their potential for efficient NOM removal [15–18]. Pre-deposition, in which an adsorbent layer is deposited on the membrane surface prior to application of the feed solution, was confirmed to be a promising process design [19–22]. Due to the fact that the pre-deposited PAC layer is always in contact with water of the maximum NOM concentration (c_0), higher loadings and efficient utilization of adsorption capacities can be achieved compared to other approaches such as continuous dosing or pre-adsorption, in which the water is contacted with and then separated from the adsorbent before it is applied to the membrane [19].

However, while generally good NOM removal rates can be achieved, results on the impact of pre-adsorption on reversible and irreversible fouling vary widely and are in part contradictory. While some studies found a higher permeate flux and better reversibility [23–25], other studies reported no significant [18] or even worse fouling when PAC was applied prior to porous membranes [26,27]. Entrapment and plugging of organic colloids in adsorbent cakes are often associated with increased filtration resistance [22,26–28]. In addition, the capability of PAC for macromolecular NOM fractions is stated to be crucial for mitigation of fouling [16,29].

This emphasizes the importance of the knowledge of the fouling potential of certain NOM fractions on the one hand and the impact of PAC's structural properties (e.g., particle size, pore distribution, inner surface area) on the ability to remove these substances on the other hand. Regarding the particle size, Matsui et al. (2011) showed that decreasing the particle size can improve both the adsorption kinetic and capacity of PAC for the adsorption of NOM in a combined PAC-UF application [30]. Similar effects were reported by Cai et al. (2013) [22], who also reported a reduction of fouling by pre-deposition of PAC. However, under certain conditions, submicron adsorbents may significantly increase fouling and lower hydraulic reversibility when combined with NOM [22,28].

While good correlations were shown for the removal of small molecular weight trace organics relative to the total surface area of PAC, the adsorption of NOM is reported to also be dependent on the pore size distribution of PAC. Due to greater molecular masses, the main portion of NOM (>2 kDa) was observed to not diffuse into the micro-porous structure of PAC; rather, adsorption takes place in a shell around the external surface of PAC particles [30–32]. Other studies stated the meso-porous surface was responsible for the main accumulation of NOM [33,34]. However, in the actual literature, there is still a lack of systematic investigation and comparison of the impact of PAC's structural properties on its potential to prevent organic fouling during combined PAC-UF.

In the current study, three commercially available PACs as well as two mechanically ground PACs were comprehensively characterized regarding their structural properties (i.e., particle size, pore size distribution, external and internal surface area). Subsequently, equilibrium isotherms as well as ultrafiltration tests with pre-deposition of PACs were performed using groundwater with a high NOM content. Finally, it was investigated which carbon characteristics correlate with PAC's efficiency for the removal of certain NOM fractions on the one hand, and the potential to reduce total and irreversible fouling during combined PAC-UF on the other hand. While the impact of individual structural properties (e.g., particle diameter, inner surface area, pore size distribution) was extensively discussed in former studies, to our best knowledge, there is no study that systematically correlates different structural properties of several PAC products with the resulting impact on NOM removal and fouling reduction in a combined PAC-UF process. In order to produce or select appropriate carbon for combined PAC-UF, knowledge of the impact of PAC's structural properties on the ability to remove specific organic foulants is of great importance. Results from the present study can help to gain a deeper understanding of the effect of pre-treatment by adsorption on low-pressure membrane fouling and will allow a reliable process design.

2. Materials and Methods

2.1. Feed Water

Experiments were conducted on northern German groundwater after treatment by aeration and rapid sand filtration for iron and manganese removal. In addition to standard parameters (pH value, electrical conductivity (EC), ion concentration), quality and quantity of NOM were determined by measurement of total and dissolved organic carbon (TOC; DOC), specific light absorption at 254 and 436 nm (UVA₂₅₄; SAC₄₃₆) and size exclusion chromatography (LC-OCD-UVD). Table 1 summarizes the feed water quality. Feed water was stored at 4 °C in the dark after sampling and before use for analysis or experiments. Prior to the experiments, the required water volume was brought to room temperature.

Table 1. Feed water quality during experiments of combined PAC-UF and for adsorption isotherms (average values with standard deviations concerning 2 to 16 measurements).

pH	EC	TOC	DOC	DOC (HS) ¹	UVA ₂₅₄	SAC ₄₃₆	SUVA	Ca ²⁺	Turb.
-	μS cm ⁻¹	mg L ⁻¹	mg L ⁻¹	mg L ⁻¹	m ⁻¹	m ⁻¹	L m ⁻¹ mg ⁻¹	mg L ⁻¹	NTU
7.9	410	3.49 ± 0.12	3.38 ± 0.10	2.24 ± 0.12	15.4 ± 0.08	1.19 ± 0.012	4.57	26.1	0.21

Note: ¹ Dissolved organic carbon content of humic substance peaks determined by LC-OCD-UVD measurements using ChromCALC Software (DOC Labor Dr. Huber (Karlsruhe, BW, Germany)) for peak integration.

To further characterize the size distribution of NOM contained in the feed water, a fractionation by membranes with defined molecular weight cut-offs (MWCO) of 150 and 20 kDa (polyether sulfone; Mycrodyn-Nadir, Wiesbaden, Germany); 10, 5 and 1 kDa (cellulose acetate, Millipore, Billerica, MA, USA) and 0.4 kDa (polyamide, DOW Chemicals, Midland, MI, USA) was performed. DOC, UVA₂₅₄ and SAC₄₃₆ were determined in respective permeates.

2.2. Powdered Activated Carbons (PACs)

Raw PACs (PAC 1–3) tested in this study are commercially available. Carbons were selected according to the manufacturer's suggestions for treatment of groundwater with a high NOM content, and carbons with different source materials and structural properties were obtained. PAC 3 was wet milled in two steps to obtain two additional PACs (PAC 3.1 and 3.2) having the same source material but different particle size distributions using grinding beads (d = 2.5 mm), plates and jar made of ZrO₂. The milling time was set to 7 h for PAC 3.1 and 14 h for PAC 3.2. PACs were characterized with respect to particle size distribution, pore size distribution, total internal surface area and internal surface area distribution. In addition, adsorption isotherms with the raw water (see Table 1) were determined.

Applied methods are summarized in Section 2.5.2. Table 2 gives an overview of structural parameters of all tested PACs investigated in this study.

Table 2. Determined structural properties of all PAC products tested in this study. (PAC 3.1 & 3.2 are milled carbons from PAC3).

Parameter	Symbol	Unit	PAC 1	PAC 2	PAC 3	PAC 3.1	PAC 3.2
Source material			mixture	brown coal		brown coal	
Particle characteristics							
Diameter (30% undersize) ¹	d ₃₀	μm	2.65	3.12	5.31	1.87	1.56
Diameter (50% undersize) ¹	d ₅₀	μm	3.59	4.37	10.30	2.97	2.50
Diameter (70% undersize) ¹	d ₇₀	μm	5.00	5.93	27.01	3.90	3.43
Specific surface area ²	s _v	μm ^{−1}	1.18	1.16	0.30	1.94	2.24
Pore structure							
Meso-pore surface	s _{p,meso}	m ² g ^{−1}	351	471	288	256	271
Meso-pore volume	v _{p,meso}	cm ³ g ^{−1}	0.51	0.66	0.50	0.64	0.88
Meso-pore radius	r _{p70,meso}	Å	25.8	25.2	29.0	29.9	35.4
Micro-pore volume	v _{p,micro}	cm ³ g ^{−1}	0.26	0.24	0.04	0.07	0.07
Internal surface area							
Total surface area	s _{B.E.T.}	m ² g ^{−1}	1245	1489	1257	1099	1071

Notes: ¹ Quantiles related to the particle volume distribution; ² Specific surface area s_v corresponds to the ratio between particle's external surface area per particle volume (μm²/μm³ = μm^{−1}).

2.3. Ultrafiltration Set-Up and Membrane

Lab-scale filtration experiments were conducted using unstirred Amicon 8200 filtration cells manufactured by Millipore (Billerica, MA, USA). Ultrafiltration membranes (UP150, Microdyn-Nadir, Wiesbaden, Germany) made of polyether sulfone with an MWCO of 150 kDa (pure water permeability $K_w = 470 \pm 18 \text{ L m}^{-2} \text{ h}^{-1} \text{ bar}^{-1}$; contact angle $\Theta = 53^\circ \pm 2.5^\circ$) were applied. Total membrane area accounted for $2.87 \times 10^{-3} \text{ m}^2$. Membranes were soaked in pure water at 4 °C for a minimum of 24 h before being used in any experiments. Prior to use, membranes were equilibrated to room temperature ($20 \pm 1^\circ \text{C}$) and flushed with 1 L of pure water to remove any organic residues from the manufacturing process.

In all cases, new membranes were used for the filtration tests. At the beginning of each experiment, 200 mL of pure water was filtered through each membrane to determine the pure water permeability. Following this, the respective mass of PAC (stock solution concentration = 2 g/L) was suspended in 100 mL pure water and pre-deposited on the membrane surface by filtering the solution through the membrane. Afterwards, the cell was connected to the feed water reservoir ($V = 5 \text{ L}$). A pressure of 1 bar (i.e., transmembrane pressure) was then applied using nitrogen gas. Filtration proceeded in dead-end mode, at constant pressure, until 500 mL of permeate had been collected. The membranes were then backwashed by installing them upside-down in the cell using a pressure of 1 bar and 50 mL of previously generated permeate. Even though backwash intensity in real applications is normally higher, relative comparison of the potential of different PACs for fouling reduction can be made based on this experimental procedure. Once the backwash was finished, 200 mL of pure water was again filtered to determine the pure water permeability after backwash and to define the reversible and irreversible portion of fouling.

In all experiments, the mass of collected permeate was recorded at intervals of 10 s using a computer. Using the recorded masses, total (R_f), hydraulic reversible (R_{rev}) and hydraulic irreversible (R_{irr}) fouling resistance was calculated according to Crittenden et al. (2010) [35]. All experiments were carried out at room temperature ($20 \pm 1^\circ \text{C}$). Viscosity of water for calculation of resistances was normalized to a temperature of 20 °C [35].

2.4. Experimental Procedures

2.4.1. Filtration Experiments

All PACs were tested analogously on the lab-scale UF setup. To assess the fouling behavior of the raw water without adsorption and to check reproducibility, five filtration tests were conducted without pre-deposition of any PAC (reference experiments). Then, the impact of structural properties of PACs on the efficiency of NOM removal and fouling reduction was investigated by pre-depositing the respective PAC on the membrane surface in theoretical concentrations of 1 (only PAC 1 + PAC 2), 2.5 (only PAC 3), 5, 10 and 20 mg/L considering a filtration volume of 500 mL, which corresponds to a PAC mass load per membrane area of 0.17, 0.44, 0.87, 1.74 and 3.48 g/m². For the milled PACs, additional tests were conducted by applying 40 and 80 mg/L (6.97 and 13.94 g/m²). Feed and permeate were analyzed according to Chapter 2.5.1. All experiments were carried out at least in duplicate.

2.4.2. Adsorption Isotherms

Adsorption isotherms were determined according to DVGW W 239 (A) technical regulation [36] applying carbon concentrations of 0, 1, 2.5 (only PAC 3, PAC 3.1, PAC 3.2), 5, 10, 20, 50, 100 and 250 mg L⁻¹ to a batch volume of 200 mL. After a contact time of 72 h on an orbital shaker at 150 rpm, which was proved to be sufficient to reach equilibrium since no further change in concentration took place, PAC was separated using a 0.45-μm polypropylene syringe filter (VWR, Radnor, PA, USA). The Freundlich isotherm model was applied for data fitting.

2.5. Analytical Methods

2.5.1. Water Analysis

The composition of feed and permeate samples was characterized using total organic carbon analysis (TOC-V CSM total organic carbon (TOC) analyzer, Shimadzu, Kyoto, Japan) as well as specific light absorption at 254 nm (UVA₂₅₄) and 436 nm (SAC₄₃₆) (DR5000 UV-vis spectrometer, Hach-Lange, Düsseldorf, Germany). Size distribution of the dissolved organic water constituents was determined by size exclusion chromatography with organic carbon and UV detection (liquid chromatography–organic carbon detection–UV detection (LC-OCD–UVD), DOC Labor Dr. Huber (Karlsruhe, Germany), column HW-50S (Toyoparl, Griesheim, Germany) as described by Jantschik et al. [37]. For all measurements, samples were pre-filtered using a 0.45-μm polypropylene syringe filter (VWR, Radnor, PA, USA). Any samples that could not be analyzed immediately were stored at 4 °C in the dark. All analyses were carried out at least in triplicate.

2.5.2. Carbon Analysis

The applied three raw PACs as well as two wet milled PACs were characterized regarding their structural properties (e.g., particle size and morphology, pore structure, BET surface area).

Laser Obscuration Time Principle using the EyeTech device (Ankersmid, Nijverdal, The Netherlands) and the corresponding analysis software were applied to examine particle size distribution of PACs. For this work, the laser lens A100 and ACM-101 Magnetic Stirring Cell was employed, using disposable plastic cuvettes with a length of 1 cm. The PACs were applied as ultra-pure water suspensions (Milli-Q). For each sample, three measurements were conducted, each lasting until a confidence of 98% was reached. For further information see Jantschik et al. (1992) [38].

Pore size analyses were performed using a Quantachrome ASiQwin (Quantachrome Instruments, Boynton Beach, FL, USA) and the corresponding software. Nitrogen was used as analysis gas (at 77.35 K). Prior to the measurement, samples were degassed for at least 3 h at 300 °C. The isotherm data were analyzed with respect to the specific B.E.T.-surface (B.E.T. method), micro-pore volume (s-method) and the pore size distribution in the meso-pore range (BJH-method) [39]. For nitrogen,

a relative molecular mass of 28.013, a molecular cross section of 16.2 Å and a liquid density of 0.808 g cm^{−3} were assumed.

3. Results and Discussion

3.1. Ultrafiltration

This section illustrates results of UF experiments without pre-deposition of PACs. It covers the effect on sole UF on rejection of certain NOM fractions; in the second part, the impact of filtration without adsorptive pre-treatment on the UF performance is displayed.

3.1.1. NOM Removal

In this study, treated groundwater with a high NOM content (see Table 1) was filtered by a membrane with an MWCO of 150 kDa made of PES. Figure 1a presents the LC-OCD-UV chromatograms of raw water (feed) and the respective permeate.

The chromatogram of the raw water indicates a broad molecular weight distribution of organic constituents, containing typical NOM-fractions (biopolymers, humic substances, building blocks, low molecular weight acids and neutrals) present in natural waters [37]. The dominating fraction is humic substances, the portion of which relative to total DOC accounts for 65% and corresponds to a relatively high UV-absorption ($\text{UVA}_{254} = 15.4 \pm 0.08 \text{ m}^{-1}$) and yellow color ($\text{SAC}_{436} = 1.19 \pm 0.012 \text{ m}^{-1}$) of the water. Determination of size distribution of organic bulk parameters by fractionation indicates that main the DOC fractions ($\approx 87\%$) have molecular masses <1 kDa (Figure 1b). However, UV-absorbance and color are caused by higher molecular weight fractions. Note that 13% of the DOC contributes to 54% and 65% of the UVA_{254} and SAC_{436} , respectively, which can be related to an increasing amount of aromatic structures and conjugated double bonds with increasing molecular weight [8,37].

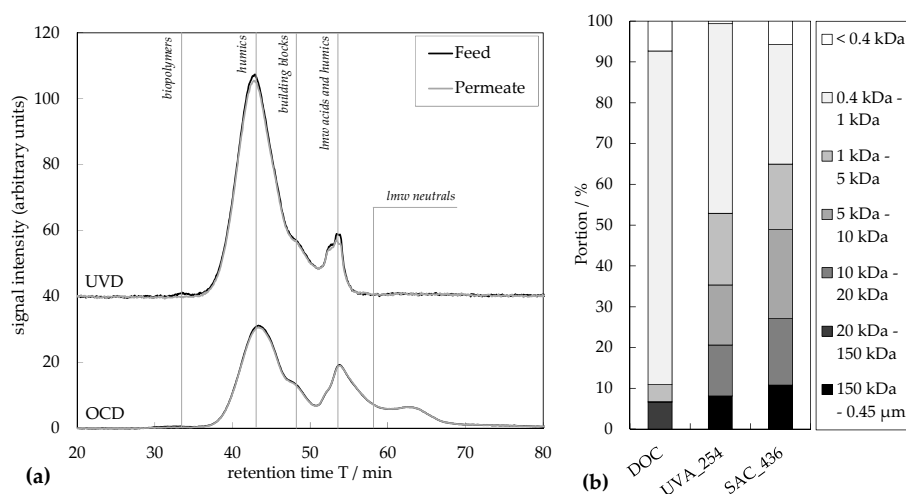


Figure 1. (a) LC-OCD-UV chromatogram of feed water and permeate after filtration by a 150-kDa UF membrane without addition of PAC containing typical DOC fractions according to Huber et al. (2011) [37]; (b) Size distribution of organic bulk parameters (DOC, UVA_{254} and SAC_{436}) of the feed water determined by fractionation by applying membranes with different MWCOs.

Due to the relatively high MWCO, the average NOM rejection of the applied UF membrane is low and accounts for 2%, 4% and 9% for DOC, UVA_{254} and SAC_{436} , respectively ($n = 5$). The LC-OCD-UV chromatograms of the permeate show that only small amounts of humic substances ($t_R \approx 43 \text{ min}$) as well as the so-called biopolymers ($t_R \approx 34 \text{ min}$) are removed (Figure 1a). The biopolymer peak is generally related to high molecular weight fractions (>10 kDa), which could be either proteins and polysaccharides or supramolecular agglomerates of humic substances as reported by Piccolo (2001) [40].

3.1.2. Membrane Fouling by NOM

Five filtration experiments of the raw water without PAC addition were conducted to check reproducibility of fouling development and to gain reference values for total as well as hydraulic reversible and irreversible fouling resistance (Figure 2).

Filtration experiments showed a good reproducibility and ended up with a fouling resistance of $1.93 \pm 0.24 \times 10^{11} \text{ m}^{-1}$ (99% confidence interval) after filtration of 500 mL of the raw water. Because the turbidity of the raw water (0.21 NTU) was low, fouling by particulate matter is assumed to be negligible. Even though only a small amount of NOM is rejected by sole UF, this amount causes a notable permeability loss during filtration of the groundwater. As derived by the rejection data, observed fouling is attributed to the macromolecular fraction of NOM carrying a high amount of UV-absorbance and color. Fouling by these fractions may occur by pore blockage on the one hand, as well as by adsorption onto and into the membrane matrix due to hydrophobic interactions with the polymeric membrane material on the other hand [8].

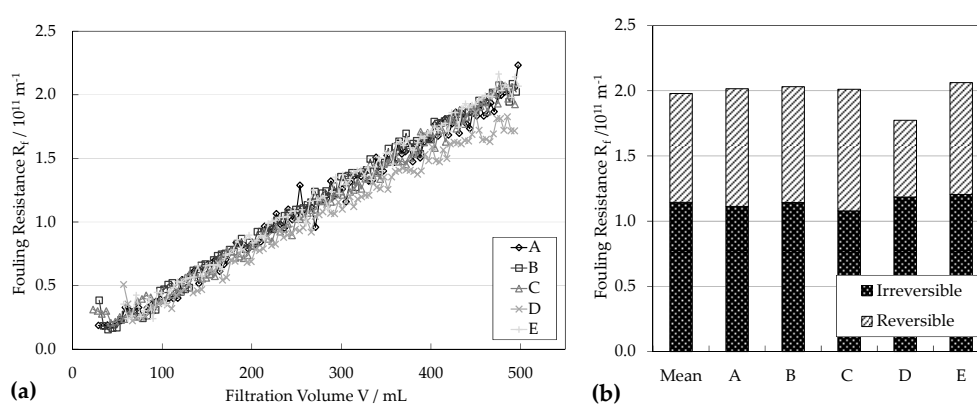


Figure 2. Reference fouling experiments: Ultrafiltration without pre-adsorption (five repetitions) (a) Fouling resistance development during filtration of 500 mL raw water; (b) Hydraulic reversible and irreversible resistance after filtration of 500 mL raw water. (Membrane: 150 kDa; PES; $2.87 \times 10^{-3} \text{ m}^2$)

With respect to the hydraulic reversibility, almost 60% of the fouling cannot be removed by hydraulic backwash. Average hydraulic irreversible resistance accounted for $1.15 \pm 0.11 \times 10^{11} \text{ m}^{-1}$ (99% confidence interval) for the five filtration trials conducted. The average total, reversible and irreversible fouling resistance will be taken as a reference and will be displayed in the next section as “0 mg PAC/L” for comparison and evaluation of the effect of PAC pre-deposition.

3.2. NOM Adsorption onto PAC

To assess the maximum adsorption capacity for NOM, adsorption isotherms ($t_R = 72 \text{ h}$) were determined for all tested carbons with respect to organic bulk parameters DOC, UVA_{254} and SAC_{436} (Figure 3). The Freundlich isotherm model was fitted to the data of each carbon. This was done for general comparison, although single-component isotherm models (e.g., Freundlich) may not be suitable for adsorption behavior of multi-component systems such as NOM in water.

Among the raw carbons (PAC 1–PAC 3), PAC 2 showed the highest adsorption capacity for all tested parameters, whereas PAC 1 and PAC 3 exhibits similar equilibrium loadings and progressions of the adsorption isotherms on a lower level (Figure 3). Differences in adsorption capacity seem to correspond to variations in total inner surface area (B.E.T.) between the raw carbons. While, for PAC 1 and PAC 3 comparable values were determined (1245 and $1257 \text{ m}^2 \text{ g}^{-1}$), PAC 2 carries a substantially higher internal surface of $1489 \text{ m}^2 \text{ g}^{-1}$. LC-OVD-UVD results indicate that all raw PACs have the highest affinity for medium molecular weight fractions (see Figure A1 in Appendix A). Building blocks, low molecular weight humics and acids are almost completely removed at moderate

PAC dosages; whereas even at the highest tested concentration (100 mg PAC/L), a certain amount of humic substances remains in solution. At 100 mg PAC/L, only minor removal was observed for the macromolecular fractions eluting as a biopolymer peak in LC-OCD-UV measurement. Due to its high molecular weight, diffusion of this fraction to the carbon particles surface as well as into its porous structure could probably be limited so that competition with medium molecular weight NOM fractions suppresses the adsorption of macromolecular constituents.

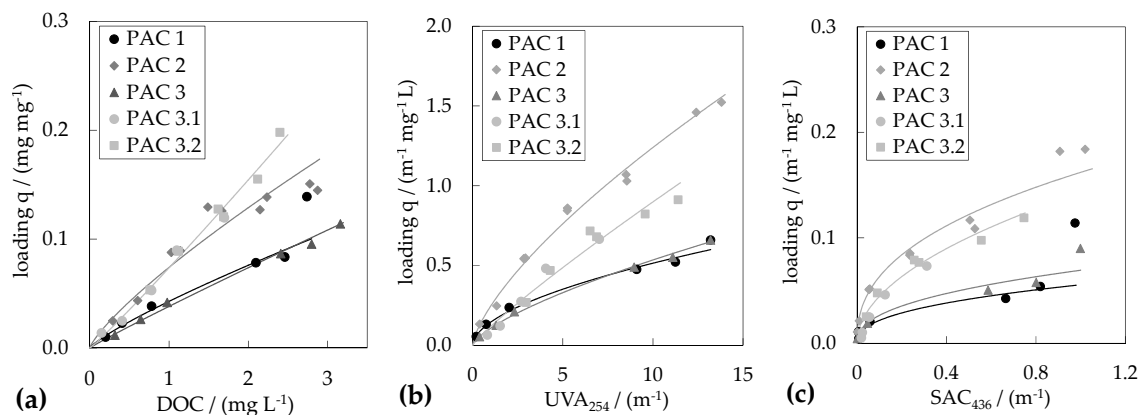


Figure 3. Adsorption isotherms of all tested PACs with respect to (a) DOC, (b) UVA₂₅₄ and (c) SAC₄₃₆. Fitted Freundlich isotherms were added for PAC 1, PAC 2, PAC 3 and PAC 3.2 to guide the eye. (T = 20 °C, V_{batch} = 200 mL, t_R = 72 h at 150 rpm).

Ground PACs (PAC 3.1 and PAC 3.2), which were produced by wet-milling of PAC 3, showed significantly higher equilibrium loadings compared to the raw carbon for all tested parameters. This is remarkable since the determined internal surface area did not increase by reducing the particle size. Such a behavior could be related to different effects: On the one hand, due to the grinding, additional inner pore structures become available for NOM adsorption that have not been accessible before, while pore size generally increases indicated by a higher meso-pore volume (see Table 2). On the other hand, the specific surface area, which corresponds to the ratio between a particle's external surface area per particle volume, of PAC is increasing. Due to diffusive limitations, particularly large organic molecules were reported to not completely penetrate PACs' inner structure but rather adsorb in a shell around the external surface of the particles [30–32]. A reduction in particle diameter will significantly increase the external surface area (see Table 2) and therefore provide larger surface for adsorption.

These results suggest that a higher inner surface area does not necessarily lead to a higher adsorption capacity for NOM. Structural parameters such as particle diameter, specific surface and pore distribution need to be considered as well for an estimation of the NOM adsorption potential and PAC selection, especially when contact time between adsorbent and adsorbate is limited as is the case for the combined adsorption-ultrafiltration. Note that water is only in contact with the PAC when permeating the thin, pre-deposited adsorbent layer on the membrane surface.

3.3. Combined Adsorption-Ultrafiltration

In this section, the potential of combined PAC-UF on NOM removal as well as on membrane fouling reduction is displayed and discussed for PACs with varying structural properties. A special focus is set on the impact of particle size on the process performance.

3.3.1. NOM Removal

During filtration experiments, each raw carbon (PAC 1–3) was pre-deposited on the membrane surface at concentrations of 1, 5, 10 and 20 mg PAC/L related to the applied filtration volume (V_F = 500 mL) during the subsequent filtration of raw water. Figure 4 illustrates the removal of DOC, UVA₂₅₄ and SAC₄₃₆ of all raw carbons relative to the applied carbon concentration.

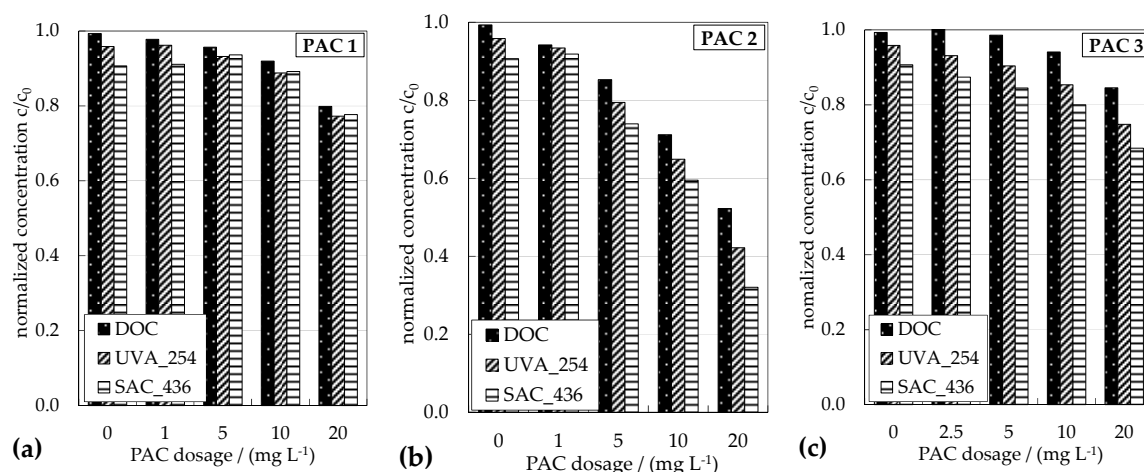


Figure 4. Ultrafiltration with pre-deposition of raw PACs in varying concentrations. Normalized average concentration of DOC, UVA₂₅₄ and SAC₄₃₆ dependent on applied carbon concentration of (a) PAC 1, (b) PAC 2 and (c) PAC 3. (Membrane: 150 kDa; PES; $2.87 \times 10^{-3} \text{ m}^2$; $V_F = 500 \text{ mL}$; $n = 2-3$).

Due to pre-deposition of PAC, NOM rejection increases compared to sole UF. The higher the mass of PAC applied, the higher the removal of NOM bulk parameters during combined PAC-UF. Comparing the raw PACs, similar trends in terms of NOM removal as seen for the equilibrium conditions were found during combined PAC-UF trials. PAC 2, which showed the highest adsorption capacity for NOM, also performed best in filtration experiments and removed 48%, 68% and 78% of DOC, UVA₂₅₄ and SAC₄₃₆, respectively, at the highest carbon dosage (20 mg/L). Applying equal concentrations, PAC 1 and PAC 3 showed significantly lower removal rates of 20–25% and 15–32%, respectively, depending on the bulk parameter. For all carbons, rejection of SAC₄₃₆ and UVA₂₅₄ exceeds the removal of TOC. This can be related to a higher affinity of activated carbon to aromatic structures due to its low polarity and resulting hydrophobic interactions [14]. However, molecules carrying high aromaticity tend to also have higher molecular weights and, therefore, are limited in pore-diffusion [33,34].

3.3.2. Membrane Fouling

For the respective experiments, impact of pre-deposition of raw PACs on the UF surface on the filtration behavior was investigated by determining the total, hydraulic reversible and hydraulic irreversible fouling resistance after filtration of 500 mL of the raw water (Figure 5).

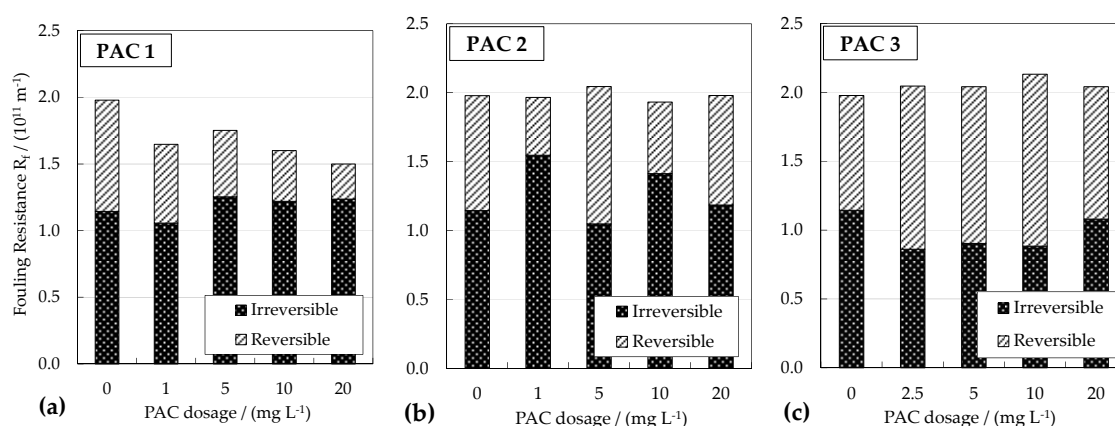


Figure 5. UF with pre-deposition of raw PACs: Average hydraulic reversible and irreversible fouling resistance after filtration of raw water with pre-deposition of (a) PAC 1, (b) PAC 2 and (c) PAC 3 in varying concentrations. (Membrane: 150 kDa; PES; $2.87 \times 10^{-3} \text{ m}^2$; $V_F = 500 \text{ mL}$; $n = 2-3$).

The additional cake resistance caused by PAC particles can be neglected compared to the resistance induced by the membrane itself [28], which explains why PAC addition in the tested range did not cause any significant increase in resistance in any of the experiments conducted. Contrary to expectations, differences in NOM removal between the tested carbons are not in line with the resulting filtration behavior. Applying PAC 2, which showed the highest NOM rejection, neither an impact on total fouling resistance development nor a clear tendency with respect to its reversibility was observed. Hydraulic reversible and irreversible resistance stayed in the same range as that detected for the filtration without adsorption. A similar tendency holds true for PAC 3, which had no impact on filtration performance as it could have been expected by considering the NOM removal rates.

In contrast, PAC 1, which showed a similar removal of organic bulk parameters as PAC 3, showed a decreasing total fouling resistance with increasing PAC dosage. Fouling resistance at 20 mg PAC/L accounted for $1.50 \times 10^{11} \text{ m}^{-1}$, which corresponds to a reduction of 25%. Based on the structural properties of the PACs tested, it becomes apparent that the main difference between PAC 1 and the other two raw carbons is the mean particle diameter (d_{50}). For PAC 1, this was determined to be $3.6 \mu\text{m}$, whereas for PAC 2 and PAC 3, it was $4.4 \mu\text{m}$ and $10.3 \mu\text{m}$, respectively. Since external surface increases over-proportionally with decreasing particle diameter, this leads to a considerably higher external surface area where macromolecular NOM fractions that were identified to be the main reason for fouling during UF of the tested water (see Section 3.1.2) might be able to adsorb. However, for PAC 1, no significant decrease of the hydraulic irreversible fouling was observed.

3.3.3. Impact of Particle Size

PAC 3 ($d_{50} = 10.3 \mu\text{m}$) was wet-milled in two steps to obtain additional PACs from the same raw material but having different particle sizes. Mean particle diameter (d_{50}) accounted for $2.97 \mu\text{m}$ for PAC 3.1 and $2.50 \mu\text{m}$ for PAC 3.2 (see Table 2). UF tests were performed with pre-deposition of these PACs at concentration of 10, 20, 40 and 80 mg/L with respect to a filtration volume of 500 mL of the raw water. According to expectations, increasing PAC dosage leads to increasing removal of all NOM bulk parameters (Figure 6). However, compared to the raw carbon (PAC 3), considerably higher removal rates were achieved by milled carbons when the same carbon concentration was applied. Whereas PAC 3 resulted in a removal of 15% and 32% for DOC and SAC_{436} , respectively, carbon with the smallest particle diameter (PAC 3.2) achieved a removal 47% and 81% at a dosage of 20 mg/L.

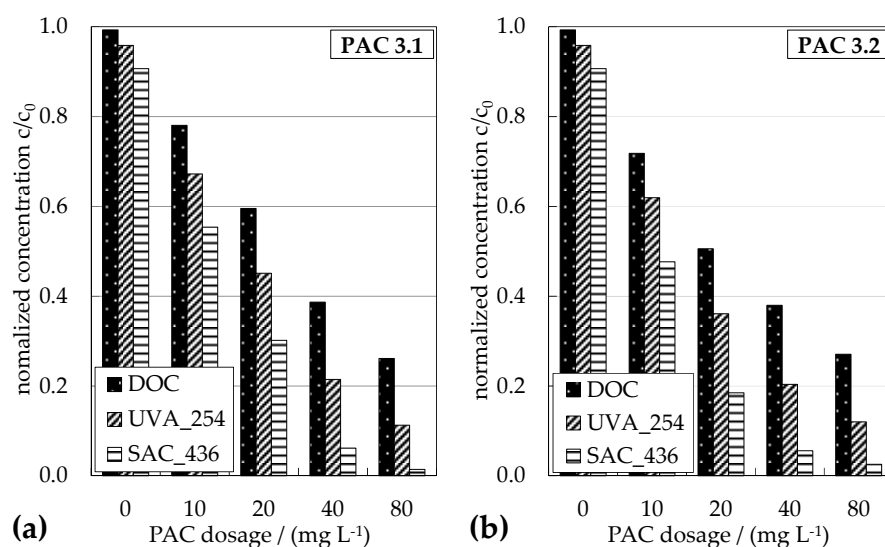


Figure 6. Ultrafiltration with pre-deposition of milled PACs at varying concentrations. Normalized average concentration of DOC, UVA₂₅₄ and SAC₄₃₆ dependent on applied carbon concentration of (a) PAC 3.1 and (b) PAC 3.2. (Membrane: 150 kDa; PES; $2.87 \times 10^{-3} \text{ m}^2$; $V_F = 500 \text{ mL}$; $n = 2-3$).

Independent of the bulk parameter, NOM removal increases with decreasing particle diameter (rejection: PAC 3.2 > PAC 3.1 > PAC 3). This might be attributed to a higher external surface area and a better accessibility to meso-pores for organic molecules (see Section 3.2). However, differences of removal rates between raw PAC and milled PACs are even more pronounced as expected based on adsorption isotherms. Applying the same PAC mass but with smaller particle sizes in combined PAC-UF additionally seems to enhance the mass transport and kinetic of adsorption due to a more homogeneous PAC distribution on the membrane surface (higher amount of surface coverage per mass of particles) and favorable hydrodynamic conditions. Furthermore, the relation between the removal of different organic bulk parameters is different between the raw carbon and the milled carbons. Compared to total organics (DOC), removal of UVA₂₅₄ and, particularly, SAC₄₃₆ is more distinct for the milled PACs than observed by applying the raw carbon. This gives further evidence that a larger portion of high molecular weight fractions carrying structures that are more aromatic are better able to adsorb when particle diameter is decreased. This could be favorable for fouling mitigation since these fractions were shown to cause the main permeability loss when filtering the raw water.

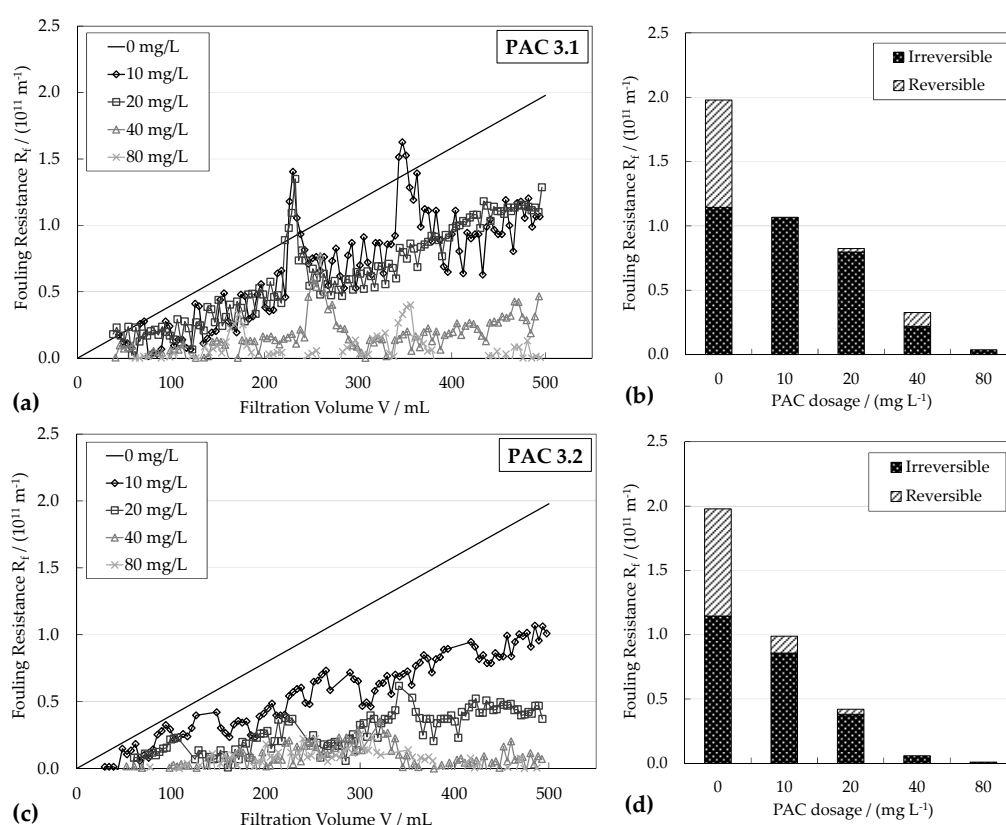


Figure 7. Ultrafiltration with pre-deposition of milled PACs in varying concentrations. Left: Fouling resistance development during filtration of raw water with pre-deposition of (a) PAC 3.1 and (c) PAC 3.2. Right: Average hydraulic reversible and irreversible resistance after filtration of raw water with pre-deposition of (b) PAC 3.1 and (d) PAC 3.2. (Membrane: 150 kDa; PES; $2.87 \times 10^{-3} \text{ m}^2$; $V_F = 500 \text{ mL}$; $n = 2\text{--}3$).

Figure 7 presents the impact of pre-deposition of the milled PACs on the development of the fouling resistance (a, c) and its reversibility by hydraulic backwashing (b, d) during ultrafiltration of 500 mL of the raw water. The solid lines in the left figures represent the average fouling resistance development when raw water without addition of PAC was filtered (see Figure 2).

In contrast to the raw carbon (PAC 3) (see Figure 5), both milled PACs significantly enhanced the UF performance. Increasing PAC concentration led to a decrease in both total and hydraulic irreversible fouling resistance. The development of fouling resistance during filtration of 500 mL

raw water showed a less steep slope, which indicates less pore blocking and pore constrictions by water constituents. The irreversible fouling resistance was also lowered, which can be attributed to a rejection of macromolecular NOM in the PAC cake layer that is no longer able to contribute to fouling. Comparing both milled carbons, mitigation of fouling was more pronounced for the carbon with the lower particle diameter (PAC 3.2), which completely mitigated fouling at the highest applied concentration of 80 mg/L. It is furthermore remarkable, that even though the removal of DOC and UVA₂₅₄ was similar between PAC 3.2 and PAC 2 at the same concentrations, significantly different filtration behavior was observed. This underlines the fact that not only the mass of NOM that is removed, but more so its quality, is crucial to prevent membrane fouling by PAC-UF treatment. Lower particle sizes obviously improve the ability of high molecular weight NOM fractions to adsorb onto activated carbon surfaces. This is supported by the fact that even though removal rates of DOC and UVA₂₅₄ were similar between PAC 3.2 and PAC 2, the milled carbon achieved a significantly higher reduction of SAC₄₃₆ as a representative parameter for macromolecular NOM fractions (see also Figure 1b). This emphasizes that PACs' structural properties should exhibit high molecular weight organic removal if PAC addition is aimed at fouling mitigation in combined adsorption-UF.

3.4. Impact of PAC Properties on Process Efficiency

To systematically identify relations between PAC properties and the resulting potential to generally remove NOM on the one hand, and to reduce membrane fouling on the other hand, structural parameters of all tested PACs were correlated to DOC removal and total fouling resistance at PAC dosages of 10 and 20 mg/L (Figure 8).

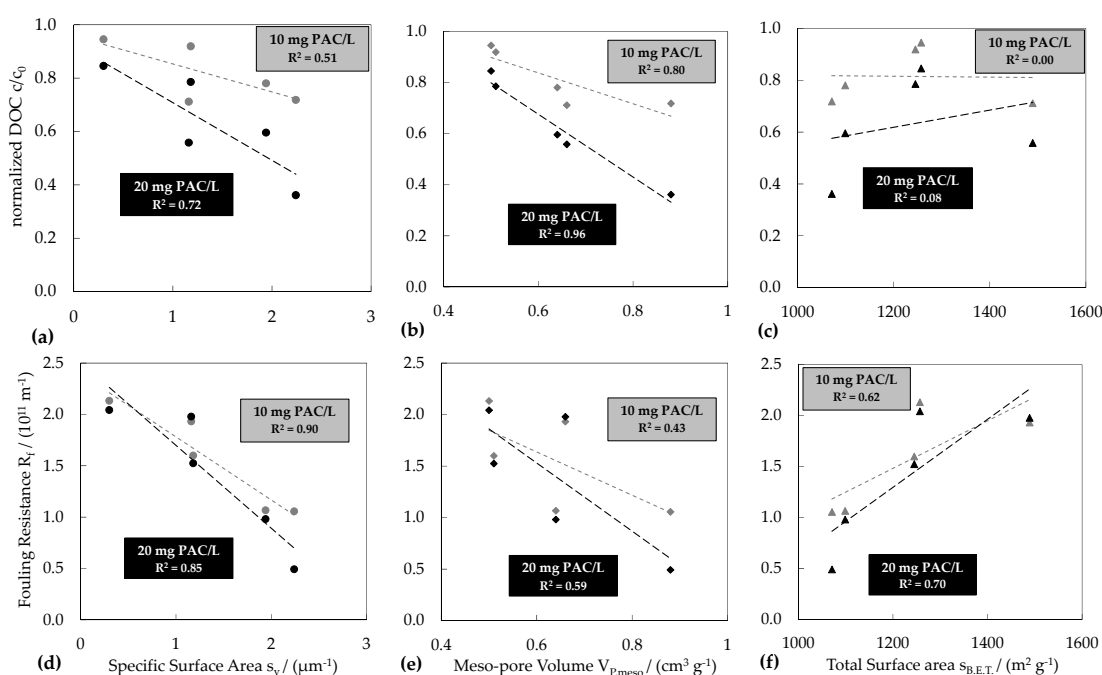


Figure 8. Normalized average DOC concentration (top) and average fouling resistance (bottom) versus (a,d) specific surface area; (b,e) meso-pore volume; (c,f) total surface area (B.E.T.) of all tested PACs with linear correlations.

Neither NOM removal nor fouling resistance showed correlations to PACs' total surface area (B.E.T.) (Figure 8c,f). In addition, classical performance indicators, such as nitrobenzene number or iodine number, showed no significant correlation to any of the parameters (results not shown). This confirms that the surface present in micro-pores, which contributes to a large portion of the total surface, does not affect NOM removal, especially if contact times are limited such as in combined PAC-UF. Previous studies showed that the main portion of organic water constituents is too large to

diffuse into the carbon micro-porous structure [30–32]. Consequently, B.E.T. surface area is not an appropriate indicator of the ability of PAC to remove NOM.

By contrast, NOM removal showed a positive correlation to the meso-pore volume (Figure 8b), which confirms adsorption takes place preferentially in larger pore structures. In addition, a higher pore volume in this range would cause a better internal mass transfer, which would also lead to a higher NOM uptake.

However, high DOC removal does not necessarily lead to better filtration behavior, which was shown in UF experiments and is confirmed by a weak correlation between meso-pore volume and the fouling resistance (Figure 8e). As already assumed in Chapter 3.3.3, the impact of particle diameter seems to be more pronounced regarding PACs' potential to reduce fouling. The external surface area increases over-proportionally with decreasing particle diameter. This leads to a higher transport of solutes through the external boundary layer, on the one hand, and to an increased number of adsorption sites for macromolecular NOM fractions that are not able to diffuse into the porous structure, on the other hand. The negative correlation between the specific surface area and the fouling resistance confirms this assumption.

However, no correlation was found between any of the structural parameters and the irreversible fouling resistance. It was shown in the previous sections that fouling of the tested raw water was induced by small amounts of high molecular weight organic substances that have high aromaticity and contribute over-proportionally to the SAC_{436} of the water. These substances have to be targeted for an efficient fouling reduction.

Figure 9 shows the total and irreversible fouling resistance in dependency on the rejection of SAC_{436} . Generally, the total fouling resistance decreases with increasing rejection of SAC_{436} . Furthermore, it becomes clear that when SAC_{436} is entirely removed, membrane fouling is almost completely prevented. Note that this corresponds to residual portions of DOC and UVA_{254} of 30% and 10%, respectively (see Section 3.3.3).

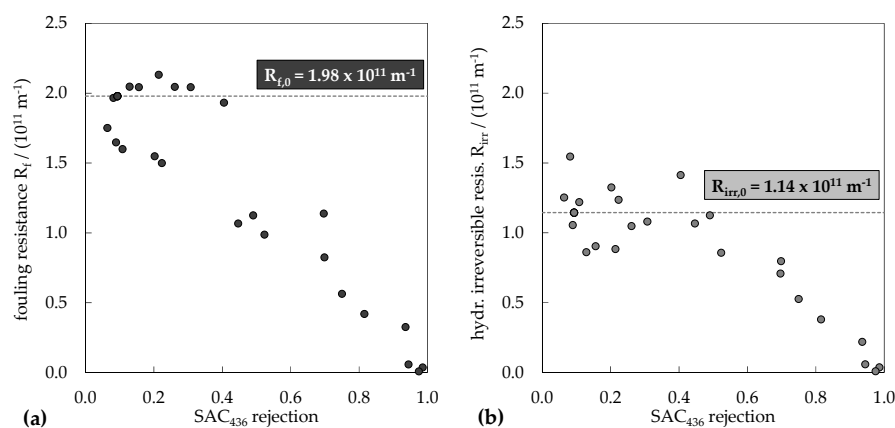


Figure 9. Impact on SAC_{436} -rejection on (a) total fouling resistance and (b) hydraulic irreversible resistance during filtration trials with all PACs tested. (Membrane: 150 kDa; PES; $2.87 \times 10^{-3} m^2$; $V_F = 500 mL$).

With respect to hydraulic irreversible fouling, it can be seen that, up to a rejection of approximately 50%, no impact of the SAC_{436} on the resulting fouling resistance is noticeable. Irreversible fouling resistance deviates around the value of the raw water without PAC addition ($R_{irr,0} = 1.14 \times 10^{11} m^{-1}$). However, when rejection for SAC_{436} exceeds 50%, hydraulic irreversible resistance undergoes linear decay to zero at a rejection of 100%. This emphasizes the hypothesis that the high molecular weight NOM fraction contributes most to membrane fouling of the applied water, and SAC_{436} gives a good indication of the fouling potential of the water. However, adsorption of macromolecular organic foulants competes with other NOM fractions, and an effective prevention of fouling only takes place when almost all SAC_{436} is removed.

4. Conclusions

The aim of this study was to investigate how PACs' structural properties affect their ability to remove NOM and reduce fouling in combined PAC-UF during treatment of groundwater with a high NOM content. Equilibrium loadings as well as UF tests with pre-deposition of three commercial PACs and two PACs milled to two smaller particle sizes were evaluated. Based on the experimental results, the following conclusions can be drawn:

- For the tested water, fouling was caused mainly by macromolecular fractions of humic substances, which carry a high amount of UV-absorbance (UVA_{254}) and yellow color (SAC_{436}).
- Conventional PAC performance indicators, such as B.E.T.-surface, iodine number, and nitrobenzene number, are not suitable to predict PACs potential for NOM removal or membrane fouling prevention because they include micro pores, which are not accessible for most NOM fractions.
- The meso-pore volume mainly governed the quantity of NOM removal and can be used to predict PACs' potential to adsorb bulk organics.
- A high DOC rejection does not necessarily lead to considerable fouling prevention; rather, the quality of DOC that is removed is crucial for resulting filtration behavior.
- To prevent fouling, PACs should be selected that are able to specifically remove humic substances with high molecular weight.
- Particle size and associated specific surface area determine PACs potential to mitigate fouling in combined PAC-UF. This is because of a more homogeneous PAC distribution on the membrane surface, a better accessibility to meso-pores for organic molecules, an enhanced transport of solutes through the external boundary layer and, particularly, a higher external surface where macromolecular foulants are able to adsorb.
- Specific light absorption at 436 nm (SAC_{436}) can serve as an indicator for the fouling potential of groundwater since it represents the macromolecular NOM fraction of the water.

This study clearly points out that structural properties of PAC are dramatically influencing the efficiency for NOM removal and fouling prevention in a combined PAC-UF process. This should be considered for PAC selection and during the design of this specific process.

Author Contributions: M.S. and S.B. conceived and designed the experiments; S.B. performed the experiments; M.S. and S.B. analyzed the data; M.S. wrote the paper.

Conflicts of Interest: The authors declare no conflict of interest.

Appendix A

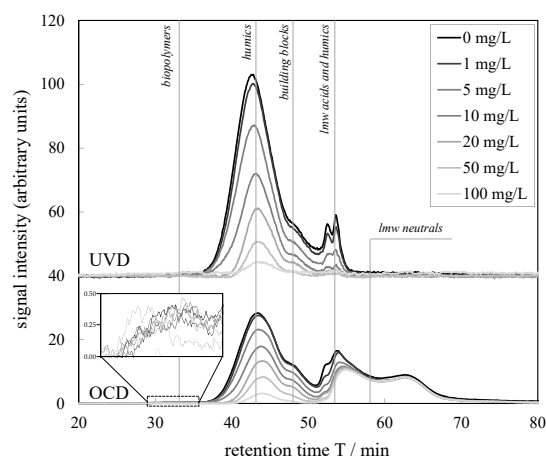


Figure A1. LC-OCD-UVD chromatogram the raw water treated by different concentrations of PAC 2 with corresponding removal of DOC fractions according to Huber et al. (2011) [37] during determination of adsorption isotherms ($T = 20\text{ }^{\circ}\text{C}$, $V_{\text{batch}} = 200\text{ mL}$, $t_R = 72\text{ h}$ @ 150 rpm).

References

1. Filella, M. Freshwaters: Which NOM matters? *Environ. Chem. Lett.* **2009**, *7*, 21–35. [[CrossRef](#)]
2. Leenheer, J.A.; Croué, J.P. Characterizing Aquatic Dissolved Organic Matter. *Environ. Sci. Technol.* **2003**, *37*, 18. [[CrossRef](#)]
3. Thurman, E.M. *Organic Geochemistry of Natural Waters*; Springer: Berlin/Heidelberg, Germany, 2013.
4. Nikolaou, A.D.; Golfinopoulos, S.K.; Lekkas, T.D.; Kostopoulou, M.N. DBP Levels in Chlorinated Drinking Water: Effect of Humic Substances. *Environ. Monit. Assess.* **2004**, *93*, 301–319. [[CrossRef](#)] [[PubMed](#)]
5. Sillanpää, M.E.T. (Ed.) *Natural Organic Matter in Water: Characterization and Treatment Methods*; Butterworth-Heinemann: Oxford, UK; Waltham, MA, USA, 2015.
6. Jacangelo, J.G.; DeMarco, J.; Owen, D.M.; Randtke, S.J. Selected processes for removing NOM: An overview. *Am. Water Works Assoc.* **1995**, *87*, 64–77.
7. Amy, G. Fundamental understanding of organic matter fouling of membranes. *Desalination* **2008**, *231*, 44–51. [[CrossRef](#)]
8. Sutzkover-Gutman, I.; Hasson, D.; Semiat, R. Humic substances fouling in ultrafiltration processes. *Desalination* **2010**, *261*, 218–231. [[CrossRef](#)]
9. Chan, R.; Chen, V. Characterization of protein fouling on membranes: Opportunities and challenges. *J. Membr. Sci.* **2004**, *242*, 169–188. [[CrossRef](#)]
10. Cho, J.; Amy, G.; Pellegrino, J.; Yoon, Y. Characterization of clean and natural organic matter (NOM) fouled NF and UF membranes, and foulants characterization. *Desalination* **1998**, *118*, 101–108. [[CrossRef](#)]
11. Evans, P.J.; Bird, M.R.; Pihlajamäki, A.; Nyström, M. The influence of hydrophobicity, roughness and charge upon ultrafiltration membranes for black tea liquor clarification. *J. Membr. Sci.* **2008**, *313*, 250–262. [[CrossRef](#)]
12. Gao, W.; Liang, H.; Ma, J.; Han, M.; Chen, Z.-L.; Han, Z.-S.; Li, G.-B. Membrane fouling control in ultrafiltration technology for drinking water production: A review. *Desalination* **2011**, *272*, 1–8. [[CrossRef](#)]
13. Katsoufidou, K.; Yiantsios, S.; Karabelas, A. A study of ultrafiltration membrane fouling by humic acids and flux recovery by backwashing: Experiments and modeling. *J. Membr. Sci.* **2005**, *266*, 40–50. [[CrossRef](#)]
14. Çeçen, F.; Aktaş, Ö. *Activated Carbon for Water and Wastewater Treatment*; Wiley-VCH Verlag GmbH & Co. KGaA: Weinheim, Germany, 2011.
15. Bhatnagar, A.; Sillanpää, M. Removal of natural organic matter (NOM) and its constituents from water by adsorption—A review. *Chemosphere* **2017**, *166*, 497–510. [[CrossRef](#)] [[PubMed](#)]
16. Haberkamp, J.; Ruhl, A.S.; Ernst, M.; Jekel, M. Impact of coagulation and adsorption on DOC fractions of secondary effluent and resulting fouling behaviour in ultrafiltration. *Water Res.* **2007**, *41*, 3794–3802. [[CrossRef](#)] [[PubMed](#)]
17. Stoquart, C.; Servais, P.; Bérubé, P.R.; Barbeau, B. Hybrid Membrane Processes using activated carbon treatment for drinking water: A review. *J. Membr. Sci.* **2012**, *411–412*, 1–12. [[CrossRef](#)]
18. Huang, H.; Schwab, K.; Jacangelo, J.G. Pretreatment for Low Pressure Membranes in Water Treatment: A Review. *Environ. Sci. Technol.* **2009**, *43*, 3011–3019. [[CrossRef](#)] [[PubMed](#)]
19. Hoffmann, G.; Hobby, R.; Gimbel, R. Organic Substance Removal by Combination of Powdered Activated Carbon Adsorption and Microfiltration—Optimization of the Process by Modifying Process Parameters. In Proceedings of the 9th IWA World Water Congress & Exhibition, Lisbon, Portugal, 21–26 September 2014.
20. Kim, J.; Cai, Z.; Benjamin, M.M. Effects of adsorbents on membrane fouling by natural organic matter. *J. Membr. Sci.* **2008**, *310*, 356–364. [[CrossRef](#)]
21. Cai, Z.; Kim, J.; Benjamin, M.M. NOM Removal by Adsorption and Membrane Filtration Using Heated Aluminum Oxide Particles. *Environ. Sci. Technol.* **2008**, *42*, 619–623. [[CrossRef](#)] [[PubMed](#)]
22. Cai, Z.; Wee, C.; Benjamin, M.M. Fouling mechanisms in low-pressure membrane filtration in the presence of an adsorbent cake layer. *J. Membr. Sci.* **2013**, *433*, 32–38. [[CrossRef](#)]
23. Lee, C.W.; Bae, S.D.; Han, S.W.; Kang, L.S. Application of ultrafiltration hybrid membrane processes for reuse of secondary effluent. *Desalination* **2007**, *202*, 239–246. [[CrossRef](#)]
24. Tsujimoto, W.; Kimura, H.; Izu, T.; Irie, T. Membrane filtration and pre-treatment by GAC. *Desalination* **1998**, *119*, 323–326. [[CrossRef](#)]
25. Matsui, Y.; Murase, R.; Sanogawa, T.; Aoki, N.; Mima, S.; Inoue, T.; Matsushita, T. Micro-ground powdered activated carbon for effective removal of natural organic matter during water treatment. *Water Sci. Technol. Water Supply* **2004**, *4*, 155–163.

26. Mozia, S.; Tomaszewska, M.; Morawski, A.W. Application of an ozonation–adsorption–ultrafiltration system for surface water treatment. *Desalination* **2006**, *190*, 308–314. [[CrossRef](#)]
27. Zhao, P.; Takizawa, S.; Katayama, H.; Ohgaki, S. Factors causing PAC cake fouling in PAC–MF (powdered activated carbon-microfiltration) water treatment systems. *Water Sci. Technol.* **2005**, *51*, 231–240. [[PubMed](#)]
28. Schulz, M.; Soltani, A.; Zheng, X.; Ernst, M. Effect of inorganic colloidal water constituents on combined low-pressure membrane fouling with natural organic matter (NOM). *J. Membr. Sci.* **2016**, *507*, 154–164. [[CrossRef](#)]
29. Lin, C.-F.; Huang, Y.-J.; Hao, O.J. Ultrafiltration processes for removing humic substances: Effect of molecular weight fractions and PAC treatment. *Water Res.* **1999**, *33*, 1252–1264. [[CrossRef](#)]
30. Matsui, Y.; Ando, N.; Yoshida, T.; Kurotobi, R.; Matsushita, T.; Ohno, K. Modeling high adsorption capacity and kinetics of organic macromolecules on super-powdered activated carbon. *Water Res.* **2011**, *45*, 1720–1728. [[CrossRef](#)] [[PubMed](#)]
31. Ando, N.; Matsui, Y.; Matsushita, T.; Ohno, K. Direct observation of solid-phase adsorbate concentration profile in powdered activated carbon particle to elucidate mechanism of high adsorption capacity on super-powdered activated carbon. *Water Res.* **2011**, *45*, 761–767. [[CrossRef](#)] [[PubMed](#)]
32. Matsui, Y.; Nakao, S.; Yoshida, T.; Taniguchi, T.; Matsushita, T. Natural organic matter that penetrates or does not penetrate activated carbon and competes or does not compete with geosmin. *Sep. Purif. Technol.* **2013**, *113*, 75–82. [[CrossRef](#)]
33. Greenwald, M.J.; Redding, A.M.; Cannon, F.S. A rapid kinetic dye test to predict the adsorption of 2-methylisoborneol onto granular activated carbons and to identify the influence of pore volume distributions. *Water Res.* **2015**, *68*, 784–792. [[CrossRef](#)] [[PubMed](#)]
34. Dastgheib, S.A.; Karanfil, T.; Cheng, W. Tailoring activated carbons for enhanced removal of natural organic matter from natural waters. *Carbon* **2004**, *42*, 547–557. [[CrossRef](#)]
35. Crittenden, J. *Water Treatment: Principles and Design*, 2nd ed.; Wiley: Hoboken, NJ, USA, 2010.
36. Deutscher Verein des Gas- und Wasserfaches e.V. *Entfernung Organischer Stoffe Bei Der Trinkwasseraufbereitung Durch Adsorption an Aktivkohle*; DVGW: Bonn, Germany, 2011.
37. Jantschik, R.; Nyffeler, F.; Donard, O. Marine particle size measurement with a stream-scanning laser system. *Mar. Geol.* **1992**, *106*, 239–250. [[CrossRef](#)]
38. Huber, S.A.; Balz, A.; Abert, M.; Pronk, W. Characterisation of aquatic humic and non-humic matter with size-exclusion chromatography—Organic carbon detection—Organic nitrogen detection (LC-OCD-OND). *Water Res.* **2011**, *45*, 879–885. [[CrossRef](#)] [[PubMed](#)]
39. Rouquerol, F.; Rouquerol, J.; Sing, K.S.W. *Adsorption by Powders and Porous Solids: Principles, Methodology and Applications*; Academic Press: San Diego, CA, USA, 1999.
40. Piccolo, A. The supramolecular structure of humic substances. *Soil Sci.* **2001**, *166*, 810–832. [[CrossRef](#)]

